Kumar, U., Mukhopadhyay, C. and Ramachandra, T.V. 2014. Cellular Automata Calibration Model to Capture Urban Growth. *Boletín Geológico y Minero,* 125 (3): 285-299
ISSN: 0366-0176

Cellular Automata Calibration Model to Capture Urban Growth

U. Kumar[1,4,5], C. Mukhopadhyay[4] and T. V. Ramachandra[1,2,3*)]

(1) Energy & Wetlands Research Group, Centre for Ecological Sciences [CES]
(2) Centre for Sustainable Technologies (astra)
(3) Centre for Infrastructure, Sustainable Transportation and Urban Planning [CiSTUP]
(4) Department of Management Studies, Indian Institute of Science, Bangalore, Karnataka, 560 012, India
Web URL: http://ces.iisc.ernet.in/energy; http://ces.iisc.ernet.in/foss
(5) International Institute of Information Technology, Bangalore-560100, India
*Author for correspondence: Energy & Wetlands Research Group [CES TE15], Centre for Ecological Sciences, New Bioscience Building, Indian Institute of Science, Bangalore 560012, India
cestvr@ces.iisc.ernet.in

ABSTRACT

Many regional environmental problems are the consequence of anthropogenic activities involving land cover changes. Temporal land cover data with social aspects are critical in tracing relationships of cause and effect on variables of interest with the effects of context on behaviour, or with the process of human environmental interaction and are also useful for the governance of urbanising cities. Many cities are now rapidly becoming urbanised and undergoing redevelopment for economic purposes with new roads, infrastructure improvements, etc. raising the necessity to understand the dynamics of the urban growth process for the planning of natural resources. Cellular automata (CA), an artificial intelligence technique based on pixels, states, neighbourhoods and transition rules is useful in modelling the urban growth process due to its ability to fit such complex spatial nature, using simple and effective rules. This study develops the calibration of a CA model by taking into account spatial and temporal dynamics of urban growth. The effectiveness of this technique is demonstrated by capturing the growth pattern of Bangalore, a city in India, with historical remote sensing and population data.

Key words: artificial intelligence, cellular automata, governance, land use model, urban growth.

Calibrado de un modelo de autómatas celulares para modelar el crecimiento urbano

RESUMEN

Muchos problemas medioambientales a nivel regional son la consecuencia de actividades antrópicas que involucran cambios en el uso del suelo. Los datos temporales de usos del suelo con aspectos sociales son críticos en el seguimiento de las relaciones causa y efecto sobre variables de interés con los efectos del contexto sobre el comportamiento, o con los procesos de interacción humana con el medioambiente y son también de utilidad para la gestión de la urbanización de las ciudades. Muchas ciudades están sufriendo, en la actualidad, una rápida urbanización y remodelación con propósitos económicos con nuevas carreteras, mejora de infraestructuras, etc. surgiendo la necesidad de entender la dinámica del proceso de crecimiento urbano para la planificación de los recursos naturales. Los autómatas celulares (AC), una técnica de inteligencia artificial basada en el uso de píxeles, estados, vecindades y reglas de transición son útiles en el modelado de los procesos de crecimiento urbano debido a su habilidad para ajustar dichos modelos espaciales complejos utilizando reglas sencillas y efectivas. Este trabajo desarrolla el calibrado de un modelo de AC teniendo en cuenta la dinámica espacial y temporal del crecimiento urbano. La efectividad de esta técnica se demuestra por la captura de los patrones de crecimiento de la ciudad de Bangalore, una ciudad de la India, utilizando datos históricos de teledetección y de población.

Palabras clave: automatas celulares, crecimiento urbano, gestión, inteligencia artificial, modelo de uso del suelo.

VERSIÓN ABREVIADA EN CASTELLANO

Introducción y metodología

La urbanización es una forma de crecimiento metropolitano con nuevas carreteras, aeropuertos, pasos elevados, centros comerciales y cualquier otra infraestructura propia del desarrollo y de la actividad económica, que afecta a la geografía física de un área. Este fenómeno está exacerbado en la India con una población urbana creciendo a un ratio de aproximadamente un 2.3% al año (Ramachandra and Kumar, 2008; World Urbanization Prospects, 2005). Este dramático incremento en urbanización ha potenciado la necesidad de entender la dinámica del proceso de crecimiento urbano a través de "modelos de crecimiento" para la distribución sostenible de recursos, la planificación y la gestión. Entre estos modelos de crecimiento, los autómatas celulares (AC) está siendo ampliamente utilizados en la simulación de procesos de crecimiento urbano, pero existen todavía aspectos no resueltos como el calibrado del modelo para una predicción fiable (Al Kheder et al., 2006, 2007; Li et al., 2001). Como los modelos de AC son sensitivos a las reglas de transición y a los valores de los parámetros, el calibrado del modelo tiene por objetivo el encontrar los mejores valores de las reglas de transición para reproducir el mismo patrón urbano que el que se obtiene a partir de datos históricos. Los objetivos de este estudio son:

- *Desarrollar e implementar un modelo de crecimiento urbano efectivo y basado en AC para simular el crecimiento como una función de la estructura de vecindad local.*
- *Desarrollar un algoritmo de calibrado que tiene en consideración las dinámicas espacial y temporal del crecimiento urbano.*

Espacialmente y temporalmente, el modelo es calibrado localmente y chequeado en la ciudad de Bangalore (estado de Karnataka en India) la cual se ha dividido en 8 direcciones o zonas diferentes Norte (N), noreste (NE), este (E), sureste (SE), sur (S), suroeste (SW), oeste (W) y noroeste (NW)) con su origen en el "centro de la ciudad" tal y como se muestra en la figura 1. Para tener un modelado de crecimiento urbano preciso, el modelo considera el efecto de los rasgos específicos del sitio y también se adapta a los cambios en los patrones de crecimiento durante el tiempo. La entrada al modelo de crecimiento urbano consiste en dos tipos de datos:

(i) Información del uso del suelo, obtenido de imágenes Landsat MSS de 1973, Landsat TM de 1992 y IRS LISS-III MS de 2006, en seis clases de interés tales como áreas residenciales, áreas comerciales, carreteras, vegetación, agua y campo abierto, a través de un clasificador supervisado basado en un algoritmo de máxima verosimilitud gausiana. Las áreas residenciales y comerciales junto a las carreteras se agruparon en una clase única llamada "urbano", de modo que la información clasificada final tiene cuatros clases de uso del suelo: urbano, vegetación, agua y campo abierto. Las clasificaciones de las imágenes de 1973, 1992 y 2006 tuvieron precisiones del 72%, 75% y 73% respectivamente y se muestran en la figura 2. Las estadísticas de las clases se ofrecen en la tabla 1.

(ii)El segundo tipo de dato de entrada ha consistido en mapas de densidad de población por distritos (unidad administrativa local básica) representada en píxeles en formato ráster para los años 1973, 1992 y 2006 que corresponden a los años de los datos de las imágenes de satélite. La figura 3 muestra el mapa de distritos (izquierda) en cada dirección y la densidad de población para cada distrito (derecha). Estos datos fueron extrapolados del mapa de densidad del Censo de Población de la India (población por distrito dividido por el área del distrito) de 1971, 1991 y 2001 utilizando curvas de ajuste cuando la densidad de población se representaba como una función de la distancia desde el centro de la ciudad, tal como se muestra en la figura 4.

El algoritmo de AC consiste en la definición de reglas de transición que controlan el crecimiento urbano, el calibrado de dichas reglas y la evaluación de los resultados para propósitos de predicción. Las reglas de transición deciden el estado del píxel en el mapa de uso del suelo de una época temporal a la siguiente, que en este caso van de 1973 a 1992 y de 1992 a 2006. El estado futuro de un píxel para el tiempo (t+1) desde el tiempo presente (t) depende de tres factores: (i) el estado actual del píxel, (ii) estado actual de los píxeles vecinos, y (iii) reglas de transición que rigen el crecimiento urbano a lo largo del tiempo. Esto sepuede representarse por:

$$S^{t+1}(\alpha) = f(S^t(\alpha), S^t(\tau), transition\_rules) \quad (1)$$

donde

$S^{t+1}(\alpha)$ *= Estado futuro del píxel* α *en el tiempo t+1*

$S^t(\alpha)$ *= Estado actual del píxel* α *en el tiempo t*

$S^t(\tau)$ *= Estado del píxel* τ *, que es un píxel vecino del píxel* α*.*

Las reglas de transición (ϕ) se diseñaron para identificar el nivel urbano requerido a la vecindad para que se urbanice un píxel de test. Las siguientes reglas fueron adoptadas de Al Kheder et al., (2007): si el píxel que está siendo transformado es agua, carretera, residencial o comercial, entonces no realizar ningún cambio; por otra parte, si el píxel pertenece a vegetación o campo abierto, entonces su estado se modifica a urbano siempre que la densidad de población sea mayor o igual al umbral (P) y el número de píxeles urbanos vecinos sea mayor o igual al umbral (R). R es un entero que va de 0 a 8 (vecindad 3x3) y P es un número real que va de 0 a 1 (con un incremento de 0.1; los valores de densidad de población se normalizaron entre 0 y 1 para cada dirección con el objeto de tener reglas de calibrado de AC efectivas). La imagen Landsat MSS clasificada más antigua (de 1973) de la ciudad de Bangalore (figura 5) obtenida a partir de la imagen del Gran Bangalore (figura 2) se utilizó como entrada al modelo de AC sobre el cual se aplicaron las reglas de transición para modelar el crecimiento urbano comenzando en esa época. Las reglas de transición de AC (ϕ) del modelo implementado fueron construidas físicamente sobre las imagenes de entrada utilizando una vecindad 3x3-$A_{i,j}^{t}$ en la ecuación (2) identifica el estado futuro del píxel de test, $a_{i,j}^{t+1}$ en la ecuación (3).

$$A_{i,j}^{t} = \begin{bmatrix} a_{i-1,j-1}^{(t)} & a_{i-1,j}^{(t)} & a_{i-1,j+1}^{(t)} \\ a_{i,j-1}^{(t)} & a_{i,j}^{(t)} & a_{i,j+1}^{(t)} \\ a_{i+1,j-1}^{(t)} & a_{i+1,j}^{(t)} & a_{i+1,j+1}^{(t)} \end{bmatrix}_{3x3neighbour} \quad (2)$$

$$a_{i,j}^{t+1} = \phi(A_{i,j}^{t}) \quad (3)$$

El calibrado (esto es, la identificación de los mejores valores para los parámetros R y P) de tales reglas se realizó espacialmente a nivel de distrito Tw (donde w representa distritos individuales) para ajustar los rasgos de la dinámica urbana local y a lo largo del tiempo para considerar los cambios urbanos temporales en cada dirección, T_t (donde t representa tiempo en años) en la ecuación (4).

$$\phi_{calibrated} = f(T_w, T_t, \phi) \quad (4)$$

ϕ en la fórmula de calibración representa el criterio seleccionado para encontrar el mejor conjunto de reglas para cierta localización espacial de distrito T_w y para una época temporal determinada T_t. Este criterio en el modelo representa el error total de modelado, esto es, el desajuste entre la salida del modelo y la realidad y que debe ser minimizado. ϕ en la ecuación (5) se definió como una función del ajuste F en la ecuación (6) y de los errores totales ΔE en la ecuación (7). Ajuste y errores totales miden la compatibilidad en términos de cantidad de urbano y patrones de urbano dentro de cada distrito con respecto a la realidad, respectivamente (Al Kheder et al., 2007).

$$\phi = Abs(F - 100\%) + \Delta E \quad (5)$$

$$F = \frac{Modeled\_urban\_count}{Ground\_truth\_urban\_count} \times 100\% \quad (6)$$

$$\Delta E = \frac{Total\_error\_count}{Total\_count} \times 100\% \quad (7)$$

Una vez que se identificaron las reglas de transición del AC y se inicializaron para cada dirección, el modelo se ejecutó desde 1973 hasta 1992.

Resultados y discusión

Los resultados de la simulación y subsecuente predicción de modelado urbano, tal y como se muestra en la tabla 2 (ver Fitness %, Total Error (ΔE %) y valores ϕ) y la figura 6 (versión ampliada) no muestran un ajuste cercano a la realidad de 1973 a 1992 en términos de cantidad de urbano, sin embargo el patrón de crecimiento urbano si se ha ajustado para diferentes direcciones hasta un cierto punto. La razón para este desajuste del número de píxeles de tipo urbano es que el crecimiento de 1973 a 1992 tuvo lugar de forma desordenada (aleatoria) y no se contabilizó en los datos del censo de población. Por consiguiente, no quedó capturado por el cambio en la densidad de población de varios distritos en diferentes direcciones. En contraste, las imágenes simuladas de 2006 (ampliada en la figura 7) están más cercanas a la imagen clasificada real en términos de patrón espacial de crecimiento urbano. Las reglas de transición para una dirección se calibraron repetidamente hasta conseguir satisfacer un criterio de convergencia. El valor medio de ajuste para la imagen de

1992 fue de aproximadamente un 60% y el error total fue de 29.09 con un ajuste aproximado del 71%. Es de destacar que para una predicción altamente precisa, el conteo urbano total modelado y el verdadero deberían coincidir y entonces la función de ajuste (F) será 1 (en tanto por uno) o 100 (en %). El error total ΔE es el error de omisión más el de comisión. A un valor mayor ΔE le corresponde un mayor porcentaje del error del conteo. Los resultados de simulación y predicción de modelado urbano, tal y como se muestra en la tabla 2 para el año 2006, muestran que los resultados de ajuste para la predicción era cercana, en términos de conteo de urbano, (valores cercano al 100%) entre los datos reales y modelados con ajuste medio de 101.60 (lo que supone una ligera sobreestimación) y el error total medio obtenido fue de 31.68%. Esto indica un nivel aproximado de ajuste del 69% en una comparación de píxel a píxel entre modelado y realidad. Por consiguiente, a valores más altos de ϕ en la ecuación (5), mayor es el error de modelado. Para la imagen simulada de 2006, el valor medio de ϕ es de 33.33, mostrando un resultado más realista comparandolo con el patrón de crecimiento urbano actual. Esto indica la habilidad del modelado y calibrado en el dominio espacial y temporal basado en AC y asimismo prueba su efectividad en la comprensión, en gran medida, de las interacciones del hombre con el medio ambiente.

Introduction

Urbanisation is a form of metropolitan growth that is a response to various economic, social, and political forces and to the physical geography of an area. This has resulted in the recent dramatic increase in urban population that is exerting an enormous pressure on the infrastructure services. Many cities are now undergoing a tremendous growth in economic activity with new roads, airports, flyovers, shopping malls, and other such infrastructure developments. This phenomena is very pronounced in India with the urban population growing at a rate of around 2.3 percent per annum (Ramachandra and Kumar, 2008; World Urbanization Prospects, 2005). An increased urban growth is irreversible due to population explosion and migration. This dramatic increase in urbanisation has raised the need to understand the dynamics of urban growth processes for planning and governance. The impact of piecemeal planning in large cities is often a major concern for stakeholders, such as those involved in researching, modelling, forecasting and policy making related to planning sustainable urban development (Barredo *et al.,* 2004). It also raises the necessity to understand the dynamics of urban growth processes through "growth models" for sustainable distribution of usable resources. Urban growth models with better understanding, prediction and visualisation capabilities have gained relevance in regional planning with increasing urbanisation in recent times as an emerging research domain. Amongst these growth models, cellular automata (CA), an artificial intelligence (AI) technique, transportation and land use planning models based on gravity theory or optimisation, spatial models (Berling-Wolff and Wu, 2004), etc. are being widely used in simulating urban growth processes apart from the conventional mathematical models (Batty and Xie, 1994; Lau and Kam, 2005). CLUE-S (the conversion of land use and its effects at small regional extent) simulates land use changes based on the empirical analyses of location suitability combined with the dynamic simulation of competition and interactions between the spatial and temporal dynamics of land use systems (Verburg *et al.,* 1999, 2002, 2004, 2010; Veldkamp, 1996). This multi-scale land use change model can predict the impact of biophysical and socio-economic forces that drive land use changes with complex spatial patterns (Verburg and Overmars, 2007; Chen *et al*., 2010; Xu *et al*., 2013). Even though the application of CA in urbanisation process modelling has been by and large successful (AlKheder *et al.,* 2006; Batty *et al.,* 1999; Cheng and Masser, 2004; Li *et al.,* 2001; Li *et al.,* 2008), there are still unresolved issues such as model calibration for reliable prediction (AlKheder *et al.,* 2006, 2007; Li *et al.,* 2001). Since CA models are sensitive to transition rules and their parameter values, calibration aims to find the best transition rule values to reproduce the same urban pattern with reference to historical data. In the literature, SLEUTH model calibration (Hagerstrand, 1967; Tobler, 1979; von Neumann, 1966; Wolfram, 1994), multi-criteria evaluation (Wu and Webster, 1998), neural networks (Li and Yeh, 2002), genetic algorithms (Alkheder *et al.,* 2006), etc. have been used for calibration. These models involve large input variables with a set of rules which are cumbersome to calibrate. Calibration of CA models requires intensive computation to select the best parameter values for accurate modelling. This study develops the calibration of a CA model by taking spatial and temporal dynamics of urban growth into account and the technique is demonstrated by capturing the growth pattern of Bangalore, a city in India with historical remote sensing (RS) and population data.

The paper is organised as follows: The section below briefly reviews the literature (focusing on the

evolution, development and calibration of CA) and states the objectives of this study, followed by data preparation (classification of RS data and generation of population density maps).This followed by an introduction to CA with the simulated results and discussion, whilst the concluding remarks are presented in the last section.

A review of the literature and objectives

AI techniques can be used to tackle complex and dynamic problems in urban studies. Wu and Silva (2010) reviewed several AI techniques that can be utilised to better understand urban and land dynamics processes as well as the associated emerging challenges. In this review we focus solely on the evolution, development and calibration of CA rules.

CA was developed in the late 1940s by S. Ulan and J. Von Neumann based on the Turing machine, placed at each cell of a lattice and connected together (Sante *et al.,* 2010). CA models for urban growth simulation have proliferated because of their simplicity, flexibility, intuitiveness, and particularly because of their ability to incorporate the spatial and temporal dimensions of the process (Sante *et al.,* 2010). The ability of CA to simulate urban growth is based on the assumption that past urban development affects future patterns through local interactions among land uses. CA-based models have abilities to fit complex spatial nature using simple and effective rules for urban simulation and are also integrated with Geographical Information Systems (Itami, 1994; Wagner, 1997) with better computational efficiency at higher spatial resolutions. Most CA models capturing the urban growth process are based on states, neighbourhoods and simple and effective transition rules that are capable of modelling the evolution of complex spatial patterns. The development of a CA model involves rule definition and calibration to produce results that are consistent with historical data. The same rules are also used for future prediction (Clarke *et al.,* 1997; White and Engelen, 1993). Sante *et al.* (2010) provide a detailed structured overview of CA models for urban growth, with new advances and the strengths and weaknesses of the different models. Wolfram (1984) demonstrated how complex natural phenomena can be modelled using CA, which laid the foundations for a theory of CA (Wolfram, 2002) on the premise that these are discrete dynamic systems wherein local interactions amongst the components generate global changes in space and time (Clarke and Gaydos, 1998). Tobler (1979) first proposed the application of cellular space models for geographic modeling. The first theoretical approach to CA-based models for the simulation of urban expansion appeared in the 1980s followed by other such studies (Batty and Xie, 1994; Couclelis, 1985; White and Engelen, 1994). Itami (1994) reviewed CA theory and its application to the simulation of spatial dynamics, and Batty (2005) provided an analysis of diverse applications for modelling urban growth using CA.

In other similar studies, Liu *et al.,* (2008) and Yang *et al.,* (2008) adopted kernel-based techniques and support vector machines (SVM) for transition rules. One of the earliest, widely used and most well-known model is CA-SLEUTH (slope, land use, exclusion, urban extent, transportation and hillshade) model (Wolfram, 1994), based on four major types of data: land cover, slope, transportation, and protected lands (Clarke *et al.,* 1997). A set of initial conditions in SLEUTH is defined by 'seed' cells which are determined by locating and dating the extent of various settlements identified from historical maps, atlases, and other sources. These seed cells represent the initial distribution of urban areas. However, the disadvantage is that sets of complex behaviour rules are developed, which involve many steps such as randomly selecting a seed location, investigating the spatial properties of the neighbouring cells, and urbanising the cell based on a set of probabilities. Silva and Clarke, (2002) used SLEUTH developed with predefined growth rules, applied spatially to gridded maps of the in a set of nested loops. Here, urban expansion was modelled in a modified two-dimensional regular grid and the problem of equifinality and parameter sensitivity to local conditions was addressed. This model is difficult to calibrate to the actual ground conditions and requires many parameters to be accounted in the development of the rules. Most of these CA models are usually designed based on individual preference and application requirements, where transition rules are defined in an ad hoc manner (Li and Yeh, 2003; Pinto and Antunes, 2007). In fact, the transition rules of a formal CA consider only the current state of the cell and its neighbours. However, a variety of factors influence urbanisation processes, such as suitability of land use, accessibility, socio-economic conditions, urban planning, etc. The transition rules of strict CA are static, although the processes that govern land use change may vary over time and space. This necessitates developing transition rules adapting to specific characteristics of each area and time interval, where the spatial and temporal variations can be achieved through calibration (Geertman *et al.,* 2007; Li *et al.,* 2008).

The discussion so far has been based on studies pertaining to the design and development of increasingly complex models and simulations of urban

dynamics that have in general ignored the process of calibration involving heuristic approaches. Most of the developed CA models need intensive computation to select the best parameter values for accurate modelling. Furthermore, calibration has largely been used for estimation and adjustment of model parameters and constants to bring the model output as close to the reality as possible. Therefore, the selection of CA transition rules remains an active research topic. This motivates development and implementation of an effective CA-based urban growth model that is easy to calibrate and which simultaneously takes the *spatial* and *temporal* dynamics of urban growth into account. The objectives of this study are as follows:

1. To develop and implement an effective CA-based urban growth model to simulate growth as a function of the local neighbourhood structure of the input data.
2. To develop a calibration algorithm that takes spatial and temporal dynamics of urban growth into consideration.

Spatially, the model is locally calibrated to take into account the effect of site-specific features whilst the temporal calibration is set up to adapt the model to the changes in the growth pattern over time. Calibration provides optimal values for transition rules to achieve accurate urban growth modelling. The input to the urban growth model consists of two types of data: (i) classified images of 1973, 1992 and 2006, where each pixel represents one of the four land use classes – urban, vegetation, water and others, (ii) population density maps represented by pixels in a raster format for the years 1973 and 1992.

CA generates transition rules for each pixel. This depends on the current state of the pixel's category (in terms of the class of land usage) and its population density value. The job of the transition rule is to decide the state of the pixel (in terms of land usage) from one time epoch to the next, which in this case happens to be from 1973 to 1992 and from 1992 to 2006.

Area of study, data and methods

This section describes the study area and input data processing scheme. The study area considered is Bangalore city, which is the principal administrative, cultural, commercial, industrial, and knowledge capital of the Karnataka state in India. The administrative jurisdiction was widened in 2006 by merging the existing area of the spatial limits of the city with eight neighbouring urban local bodies and 111 villages of Bangalore Urban District to form Greater Bangalore. Bangalore has spatially grown more than ten times from 69 to 741 square kilometres from the year 1949 to the year 2006. Now, Bangalore is the third largest metropolis in India, currently with a population of about 9.6 million (Census of India, 2011; Ramachandra *et al.,* 2008). Bangalore is composed of 100 wards or neighbourhoods. Since, urbanisation and urban sprawl are more of a local phenomenon and site specific, local urban sprawl tends to increase in a certain direction along ring roads, highways, or around service facilities in another direction, which later becomes the urban centre hub. The greater the distance from the city centre, the lesser is the development (Cheng and Masser, 2004; Li and Yeh, 2002; Yeh and Li, 2001). Therefore, a better way to understand the spatio-temporal pattern of a city is to study the urban landscape in different directions from the central business district. For this reason, in the current study, the city was divided into 8 zones [north (N), northeast (NE), east (E), southeast (SE), south (S), southwest (SW), west (W), and northwest (NW)] with their origin from the 'city centre' as shown in Figure 1. Visualisation of the sprawl process is crucial in urban planning for providing basic amenities in different geographical locations.

The two types of input data were:

(i) classified RS data of 1973, 1992 and 2006.

(ii) population density maps of 1973 and 1992.

The Landsat multispectral scanner (MSS) of 1973 (in blue (B), green (G), red (R) and near infrared (IR) bands of 79 m spatial resolution), Landsat thematic mapper (TM) of 1992 (B, G, R, near IR, mid IR-1 and mid IR-2 bands of 30 m spatial resolution), and IRS linear imaging self scanner (LISS) -III for 2006 (in G, R and NIR bands of 23.5 m spatial resolution) were used for the generation of land use maps. The data are stored in 8-bit format, i.e. each pixel can take any value from 0 to 255 (2^8= 256 values) which represents the reflectance by that pixel corresponding to the same geographical location on the ground. The 1973 image was of the dimension 429 rows x 445 columns, whereas the 1992 image was of 1130 rows x 1170 columns and the 2006 image was of 1445 rows x 1496 columns. The differences in the size of the images are due to variations in the spatial resolution of the pixels (79 m, 30 m, and 23.5 m respectively). These data were rectified and registered for systematic errors with known ground control points that were identifiable both in the image as well as in the Survey of India (SOI) Topographical sheets of 1:50000 scale and projected to a polyconic system with a geographic latitude-longitude coordinate system and Evrst56 as the datum. All data were resampled to have 23.5 m spatial resolution, having

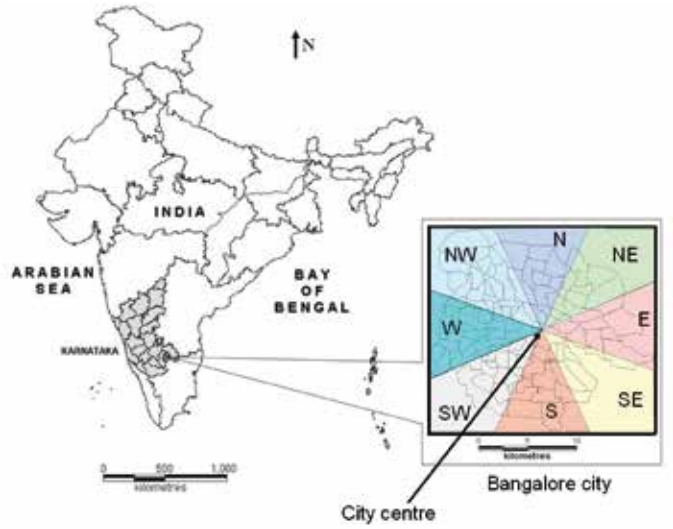

Figure 1. Study area: Bangalore city, Greater Bangalore, India.
Figura 1. *Área de estudio: ciudad de Bangalore, Gran Bangalore, India.*

1445 rows x 1496 columns to fit each other spatially. Six classes of interest were identified from the false colour composite images: residential areas, commercial areas, roads, vegetation, water and open land.

Supervised classification of the image was performed using a Maximum Likelihood classifier (MLC). MLC has become popular and widespread in RS because of its robustness (Conese and Maselli, 1992; Ediriwickrema and Khorram, 1997; Strahler, 1980; Zheng *et al.,* 2005). MLC assumes that each class in each band can be described by a normal distribution (Bayarsaikhan *et al.,* 2009). For each land use class (residential areas, commercial areas, roads, vegetation, water, and open land), training samples / polygons were collected using a hand held GPS from across the city, representing approximately 10% of the study area. With these 10% known pixel labels from training data, the aim was to assign labels to all the remaining pixels in the image (RS data of Bangalore city). The objective was to classify a pixel with M x 1 grey scale values, corresponding to M spectral bands, into one of the N spatial classes.

At the outset, let the spectral classes in the data be represented by ω_n, n=1,..., N, where N is the total number of classes, and $(\mathbf{x} \mid \omega_n): \ N(\mu_n, \Sigma_n)$. Let $\underset{\sim}{x}_1, \ldots, \underset{\sim}{x}_{m_n}$ denote the (m x 1) grey-scale values across the M spectral bands of m_n sampled pixels (observations or training samples which are independently and identically distributed (i.i.d.) random variables), belonging to the n^{th} spatial class, then

$$\mu_n = \frac{1}{m_n} \sum \underset{\sim}{x}_i (i = 1 \text{ to } M)$$

$$\Sigma_n = \frac{1}{m_n} \sum (\underset{\sim}{x}_i - \mu_n)(\underset{\sim}{x}_i - \mu_n)^T (i = 1 \text{ to } M)$$

Baye's decision theory forms the basis of statistical pattern recognition based on the assumption that the decision problem can be specified in probabilistic terms (Wölfel and Ekenel, 2005). The MLC assuming the distribution of data points to be Gaussian, quantitatively evaluates both the variance and covariance of the category's spectral response pattern (Lillesand and Kiefer, 2002), which is described by the mean vector and the covariance matrix. The statistical probability of a given pixel value being a member of a particular class is computed and the pixel is assigned to the most likely class (highest probability value).

$p(\omega_n|\mathbf{x})$ gives the probability that the pixel with observed column vector of DNs (digital numbers) **x,** belongs to class ω_n. It describes the pixel as a point in multispectral (MS) space (M-dimensional space, where M is the number of spectral bands). The maximum likelihood (ML) parameters are estimated from representative i.i.d. samples. Classification is performed according to

$$\mathbf{x} \in \omega_n \text{ if } p(\omega_n \mid \mathbf{x}) > p(\omega_i \mid \mathbf{x}) \ \forall \ j \neq n \qquad (1)$$

i.e., the pixel vector **x** belongs to class ω_n if $p(\omega_n|\mathbf{x})$ is largest. The ML decision rule is based on a normalised estimate of the probability density function (p.d.f.) of each class. MLC uses Baye's decision theory where the discriminant function, $g_{ln}(\mathbf{x})$ for ω_n is expressed as

$$g_{ln}(\mathbf{x}) = p(\mathbf{x}|\omega_n) p(\omega_n) \qquad (2)$$

Where, $p(\omega_n)$ is the prior probability of ω_n, $p(\mathbf{x}|\omega_n)$ is the p.d.f. (assumed to have a Gaussian distribution for each class ω_n) for pixel vector **x** conditioned on ω_n (Zheng *et al.,* 2005). Pixel vector **x** is assigned to the class for which $g_{ln}(\mathbf{x})$ is greatest. In an operational context, the logarithm form of (2) is used, and after the constants are eliminated, the discriminant function for ω_n is stated as

$$g_{ln}(\mathbf{x}) = (\mathbf{x} - \mu_n)^T \Sigma_n^{-1} (\mathbf{x} - \mu_n) + \ln |\Sigma_n| - 2 \ln p(\omega_n) \qquad (3)$$

where Σ_n is the variance-covariance matrix of ω_n, μ_n is the mean vector of ω_n. Equation (3) is a special case

of the general linear discriminant function in multivariate statistics (Johnson and Wichern, 2005) and used in this current form in the RS digital image processing community. A pixel is assigned to the class with the lowest $g_{in}(\mathbf{x})$ in equation (3) (Duda *et al.,* 2000; Richards and Jia, 2006; Zheng *et al.,* 2005).

Residential and commercial areas and roads were grouped into a single class called 'urban'. Final classified images thus had four land use classes – urban, vegetation, water and open land (others). The classified images of 1973, 1992 and 2006 had overall accuracies of 72%, 75%, and 73% respectively. Classification was done using the open source programs (i.gensig, i.class and i.maxlik) of Geographic Resources Analysis Support System (http://wgbis.ces.iisc.ernet.in/grass) and is displayed in Figure 2. The classified images were also verified with field visits and Google Earth images. The class statistics is given in Table 1.

Population density is a second input that is required for CA modelling. A population map of Bangalore was prepared from the Census of India data of 10-year intervals (1971, 1981, 1991, 2001). The Indian Census by the Directorate of the census operation, the Government of India (*http://censusindia.gov.in*) is the most credible source of information on demography (population characteristics), economic activity, literacy and education, housing and household amenities, urbanisation and many other socio-cultural and demographic data since 1872. Population densities for all 100 wards or neighbourhoods were computed by dividing their populations by their respective ward areas. Figure 3 shows the ward map (left) in each direction and the population density for each neighbourhood (a basic administrative unit) (right) in 1971, 1991 and 2001.

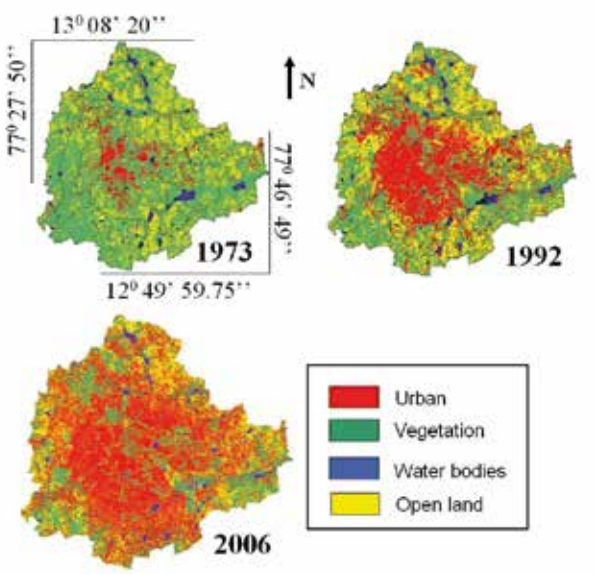

Figure 2. Greater Bangalore in 1973, 1992 and 2006.
Figura 2. *Gran Bangalore en 1973, 1992 y 2006.*

Population densities for 1973, 1992 and 2006 were extrapolated from the population densities of 1971, 1991 and 2001 to correspond with RS data. First, the centroid for each neighbourhood was calculated. Then, the Euclidean distance from each ward centroid to the city centre (see Figure 1) was computed. This process was repeated for all the wards to prepare a table of population densities versus distance. Population densities for neighbourhoods within a specified distance from the city centre were averaged to reduce the variability in data. For example, an average population density for all wards within 0-1 km was calculated then another average density was calculated for wards within 1-2, 2-3, 3-4 km and so on. Curves were fitted representing population density as a function of distance from the city centre as shown in Figure 4. The unknown model parameters in the curve fitted equations were calculated for the years 1991 and 2001. These models were used to calculate the population density for each pixel in the imagery based on its distance from the city centre for the years 1991 and 2001. The changes in model parameters over the 10 years (from 1991 to 2001) were used to calculate the yearly rate of change. The updated parameters that changed year by year were used to calculate the population density grids for the years 1973 and 1992 matching the same size of the input imagery (classified maps - 1445 rows and 1496 columns). These grids were used as input to the CA model.

Cellular automata (CA) growth modelling

This section discusses the design of CA urban growth modelling in detail. The CA algorithm consists of defining the transition rules that control urban growth, calibrating these rules, and then evaluating the results for prediction purpose.

Transition rules

Transition rules translate the effect of input data in simulating the urbanisation process. The CA algorithm design starts by defining the transition rules that drive urban growth over time. They depend on the current status of land usage and population density and are subject to certain growth constraints. The transition

Class → Year ↓		Urban	Vegetation	Water Bodies	Open land
1973	ha	5448	46639	2324	13903
	%	7.97	68.27	3.40	20.35
1992	ha	18650	31579	1790	16303
	%	27.30	46.22	2.60	23.86
2006	ha	29535	19696	1073	18017
	%	43.23	28.83	1.57	26.37

Table 1. Greater Bangalore land use statistics
Tabla 1. *Estadísticas del uso del suelo del Gran Bangalore.*

Ward No.	Ward	Distance	Density 1971	Density 1991	Density 2001
1	Vasanthnagar	1.32	400	2320	11981
2	Shivajinagar	2.11	777	3641	16252
3	Jayamahal	3.12	798	4292	18917
4	Koramangla	4.43	847	3316	23011
5	Austin Town	5.96	1925	4946	33429
6	Hebbal	6.49	273	3916	16068
7	Richmond Town	4.19	2901	9544	29139
8	Ganganagar	4.45	101	2622	23658
9	Sanjayanagar	6.24	61	3473	29221
10	J P Nagar	7.46	704	4704	19792

Figure 3. Ward map in each direction and their population densities. Distances are expressed in kilometres and population densities are expressed in persons/sq. km.
Figure 3. *Mapa de distritos en cada dirección junto a su densidad de población. Las distancias se han expresado en km y las densidades de población en personas por kilómetro cuadrado.*

rules are defined for the 3 x 3 neighbourhood of a pixel. The rules identify the neighbourhood needed for the tested cell to urbanise.

The growth constraints reflect urbanisation strategies adopted in the study area for certain land uses such as conservation of the water bodies (lakes). Urban growth in the vicinity of such sites is constrained by imposing rules that discourage urbanisation into water bodies. The future state of a pixel at time (*t+1*) from the current time (*t*) depends on three factors: (i) current state of the pixel, (ii) current states of the neighbourhood pixels, and (iii) transition rules that drive the urban growth over time, which may be represented by

$$S^{t+1}(\alpha) = f(S^t(\alpha), S^t(\tau), transition\_rules) \quad (4)$$

where

$S^{t+1}(\alpha)$ = Future state of pixel α at time epoch t+1

$S^t(\alpha)$ = Current state of pixel α at time epoch t

$S^t(\tau)$ = State of pixel τ, which is a neighbourhood pixel of pixel α.

Transition rules (ϕ) were designed to identify the required neighbourhood urban level for a test pixel to urbanise. The following rules were adopted from AlKheder *et al.,* (2007): If the pixel being transformed is either water, road, residential or commercial, then perform no change, otherwise if the pixel belongs to vegetation or open land, then its state will be altered to urban, provided the population density is ≥ threshold (*P*) and the number of surrounding urban pixels are ≥ threshold (*R*). *R* is an integer ranging from 0 to 8 (*3x3* neighbourhood) and *P* is a real number ranging from 0 to 1 (0.1 increment; population density values were normalized from 0 to 1 for each direction in order to have effective CA rules calibration).

Calibration

The calibration of urban CA model is done to determine optimal weights or parameters of the transition rules such as *P* or *R* mentioned above (Dietzel and Clarke, 2006; Li and Yeh, 2001; Li *et al.,* 2007; Stevens *et al.,* 2007; Wu, 2002). Calibration is an integral part of the CA model design and development process as it is in this step that one attempts to ensure that the model provides reasonable predictions about current and future scenarios (Li and

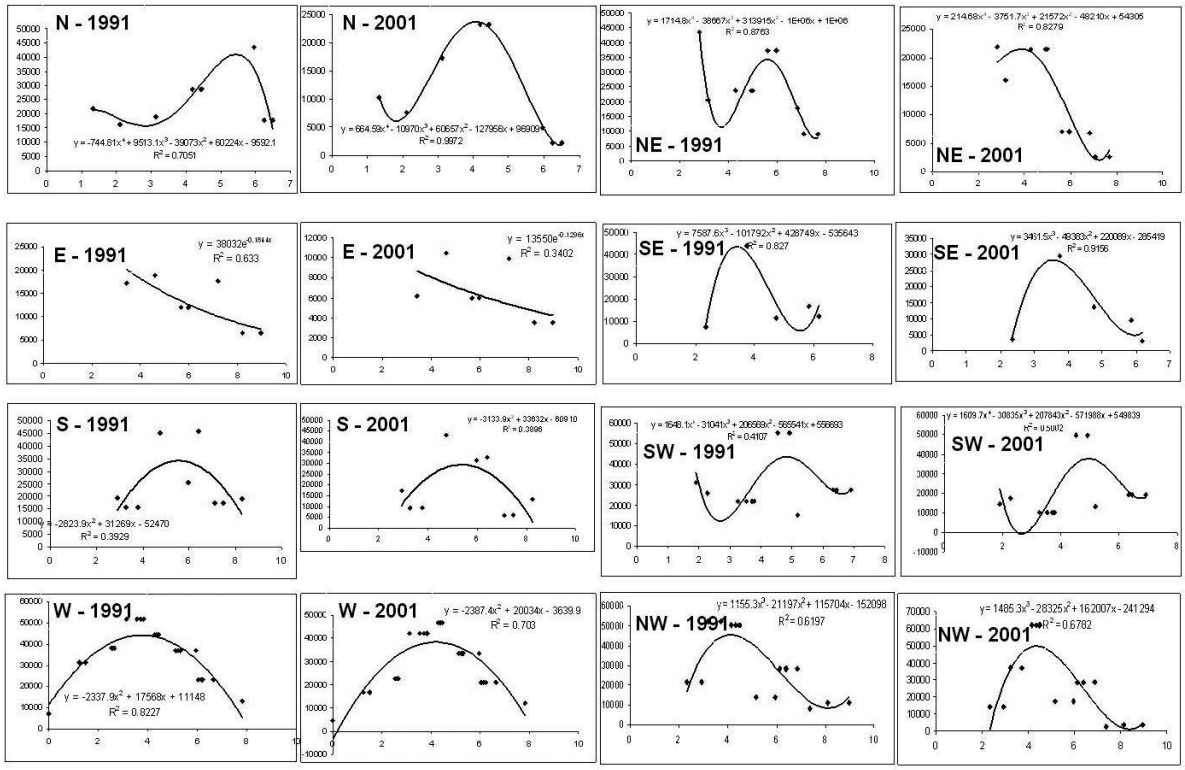

Figure 4. Direction wise population density for the year 1991 and 2001.
Figura 4. *Densidad de población direccional para los años 1991 y 2001.*

Yeh, 2001, 2002; Waddell, 2005). It aims to define the optimal set of CA rules such that the agreement between simulated results and ground truth images are as best as possible.

The relaxations allowed in CA helped to simulate more realistic urban growth that led to the emergence of a large variety of rules. To achieve this, two calibration schemes were used, namely spatial and temporal calibrations. In spatial calibration, the CA transition rules at a given time *t* were modified spatially over the 2D grid space by tuning the values of each rule set on a directional basis to match the urban dynamics for each neighbourhood with its site specific features, allowing the model to take the variability in the spatial urban growth pattern into account for realistic modelling. If the transition rules in a given direction resulted in higher growth levels (overestimated), they were modified to reduce the urban growth in that direction. In case of underestimation, the rule values of the direction under consideration were tuned to increase the amount of urban growth to match the real one. Therefore, spatial calibration is meant to find the best set of rule values that best fits a given direction according to its geographical location. This is similar to the SLEUTH model (Silva and Clarke, 2002), where the parameters can be set best that simulate the application data by narrowing both the spatial scale and the range of parameters in the calibration sequences. These parameters are then used to determine the parameter values that optimally allow the model to run into the future, i.e. to predict.

The oldest classified Landsat MSS image (of 1973) of Bangalore (Figure 5) obtained by subsetting the Greater Bangalore image (Figure 2) was used as input to the CA model over which the transition rules were applied to model the urban growth starting from this time epoch. Dividing the study area on a direction (or zones such as N, NE, E, SE, S, SW, W, and NW as explained in section 3) and further on a ward or neighbourhood basis took into consideration the effect of site specific features spatially. The same CA transition rules were defined for each direction, however, with different rule values. CA transition rules (ϕ) of the developed model were physically built over the input imagery and the rules used a 3 x 3 neighbourhood - $A_{i,j}^{t}$ in equation 5 to identify the test pixel's future state, $a_{i,j}^{t+1}$ in equation 6.

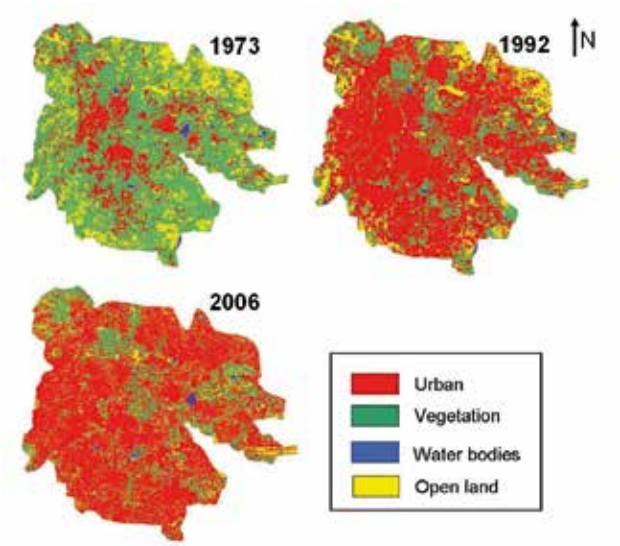

Figure 5. Bangalore city in 1973, 1992 and 2006 used in the CA model for simulation (subset of Greater Bangalore classified image).
Figura 5. *La ciudad de Bangalore en 1973, 1992 y 2006 utilizadas en el modelo AC para simulación (subconjunto de la imagen clasificada del Gran Bangalore).*

$$A_{i,j}^{t} = \begin{bmatrix} a_{i-1,j-1}^{(t)} & a_{i-1,j}^{(t)} & a_{i-1,j+1}^{(t)} \\ a_{i,j-1}^{(t)} & a_{i,j}^{(t)} & a_{i,j+1}^{(t)} \\ a_{i+1,j-1}^{(t)} & a_{i+1,j}^{(t)} & a_{i+1,j+1}^{(t)} \end{bmatrix}_{3x3 neighbourhood} \quad (5)$$

$$a_{i,j}^{t+1} = \phi(A_{i,j}^{t}) \quad (6)$$

The calibration (i.e., identifying best (*R,P*) parameter values) of such rules was performed spatially on a ward level, *Tw* (where *w* represents individual wards) to fit the local urban dynamic features and over time to consider the temporal urban changes in each direction, T_t (where *t* represents time in years) in equation 7.

$$\phi_{calibrated} = f(T_w, T_t, \phi) \quad (7)$$

ϕ in the calibration formula represents the criteria selected to find the best rule set for a certain ward spatial location T_w at a given time epoch T_t. This criterion in the model represents the total modelling errors/mismatch between modelled output and reality that need to be minimised or best matched. ϕ in equation 8 was defined as a function of fitness, *F* in equation 9 and total errors ΔE in equation 10. Fitness and total errors measure the compatibility in terms of urban count and pattern within each ward with respect to reality, respectively (Al-Kheder, *et al.,* 2007).

$$\phi = Abs(F - 100\%) + \Delta E \quad (8)$$

$$F = \frac{Modeled\_urban\_count}{Ground\_truth\_urban\_count} \times 100\% \quad (9)$$

$$\Delta E = \frac{Total\_error\_count}{Total\_count} \times 100\% \quad (10)$$

Once the CA transition rules were identified and initialised for each direction, the model was run from 1973 to 1992. The 1992 image represents the first ground truth being used for calibration. For each ward or neighbourhood, the modelling accuracy is calculated as a ratio between the simulated and real urban growth data. Over/underestimation is introduced to represent how comparable the simulated result is to the real one. This indicates how transition rules defined on a directional basis succeed in modelling the real urban growth given the predefined conditions. Calibration is meant to find the best set of rule values specific to each direction for realistic urban growth modelling.

Results and discussion

Simulation and subsequent urban modelling prediction results, as shown in Table 2 and Figure 6 (zoomed version) do not exhibit a close match to the reality from 1973 to 1992 in terms of urban count, however, the pattern of urban growth matches in various directions to some extent. The reason for this mismatch of the urban pixels is that the growth from 1973 to 1992 happened haphazardly, which was not accounted for in the population census data. Thus, they were not captured and reflected by the change in population density of various wards in different directions. In contrast, the simulated images of 2006 (zoomed in Figure 7) are closer to the real classified image in terms of the spatial pattern of urban growth.

Prediction accuracy for each direction was used as a basis for rule calibration. If a set of rules for a particular direction produced underestimated results, then it meant the growth rate was small and hence the rules were modified to increase urban growth. For overestimation, the rules were modified to reduce ur-

Direction	1973 Simulation / 1992 Prediction			1992 Simulation / 2006 Prediction		
	Fitness %	Total Error (ΔE%)	ϕ	Fitness %	Total Error (ΔE%)	ϕ
North	52.58	32.39	79.82	101.71	30.82	32.53
Northeast	66.43	30.48	64.05	101.66	35.44	37.10
East	65.51	39.82	74.31	99.87	40.68	40.81
Southeast	42.28	29.72	87.44	99.89	36.86	36.97
South	46.39	33.33	86.93	105.36	29.18	34.54
Southwest	58.55	16.71	58.16	100.58	23.24	23.81
West	61.35	17.22	55.87	100.80	21.15	21.96
Northwest	86.13	33.08	46.95	102.90	36.08	38.98
Average	59.90	29.09	69.19	101.60	31.68	33.33

Table 2. Numerical evaluation results.
Tabla 2. *Resultados de la evaluación numérica.*

ban growth. The transition rules for a direction were repeatedly calibrated till the convergence criterion was met. The classified image provides the reference for calibration process. In Table 2, the *Fitness %, Total Error (ΔE %)* and ϕ values for the year 1992 indicate a poor match of the simulated image with the real image (classified image), which is an indication of underestimation of urban pixels in various directions. However, the results for the 2006 simulated image (Table 2) indicate very good spatial prediction accuracy. The spatial variability between various directions as compared to the real image is small. This indicates the effect of spatial calibration in matching each direction with its realistic urban growth pattern through calibrating its rules. It also helped in capturing finer details, whilst calibrating the model over smaller spatial units to reduce modelling uncertainty. Visually, calibration on a directional basis succeeds in preserving the urban pattern over space and over time. The results of rule values at the end of the calibration process indicate similarity between growth in various directions, such as in the east, west and northwest. In reality, these wards have almost the same growth rate and pattern because of similar infrastructure, facilities, and more open areas for outer growth and urban sprawl. Most of these similar wards or neighbourhoods have ring roads or highways passing through them that allow linear urban growth to happen along them. The average fitness value for the 1992 image was ~ 60% and the total error was 29.09 with an approximate match of 71%. It worth noting that for a highly accurate prediction, the total modelled urban count and ground truth urban count will be equal and therefore the fitness value (*F*) will be 1 or 100%. The total error *ΔE* is the error of omission and commission. The greater the value of *ΔE,* the greater the percentage of error count is. There seems to be some mismatch between the actual and simulated urban pixel patterns in 1992 as this pattern was not captured accurately by the change in population density contours and the curve fits in various wards and different directions. Simulation and prediction urban modelling results, as shown in Table 2 for the year 2006, show that the fitness results for prediction were close in terms of urban count (values close to 100%) between the modelled and real data with average fit-

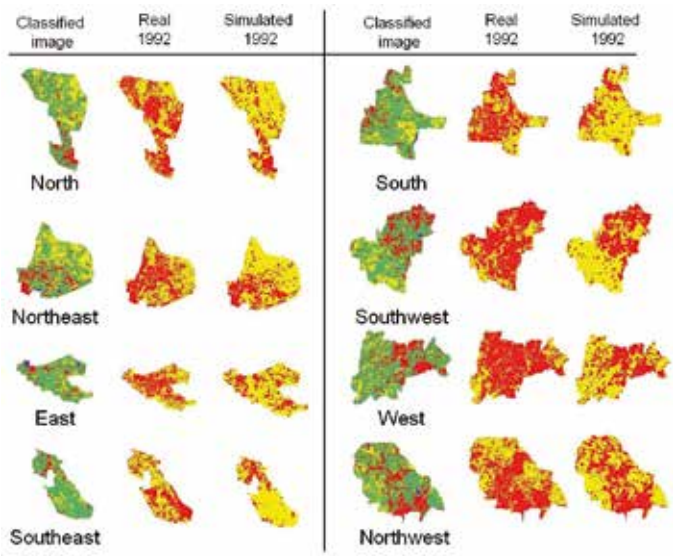

Figure 6. Classified images of 1973, real image and simulated image of 1992. Red colour indicates urban areas, yellow represents other classes (vegetation, water or open land) in real and simulated images.
Figura 6. *Imágenes clasificadas para 1973 e imágenes real y simulada para 1992. El color rojo indica las zonas urbanas y el amarillo representa las otras clases (vegetación, agua y campo abierto) tanto en las imágenes reales como en las simuladas.*

ness of 101.60 (which is a slight overestimate) and the average total error of 31.68% was achieved. This indicates an approximate match level of 69% on a pixel by pixel basis between modelling and reality. Therefore, the higher the value of ϕ in equation 8, the higher the modelling error is. For the 2006 simulated image, the average ϕ is 33.33, showing a more realistic result compared to the actual urban growth pattern. This is a high accuracy level compared to the results shown in the literature for the urban land spatial fit area that was only 28.15 to 44.6% (Yang and Lo, 2003). The close urban pattern match is also clear in Figure 7, where the simulated images have urban distribution similar to those shown in their corresponding real images. This indicates the ability of CA based modelling and calibration in spatial and temporal domains and also proves their effectiveness in understanding human-environmental interactions to a great extent. Based on the objective of this study, cell space, cell states, neighbourhoods, growth constraints, and calibration followed by validation were carried out using simple CA models for complex dynamic urban systems. The state of any cell depends upon some function which reacts to what is already in that cell as well as some function which relates the cell to what is happening in its immediate neighbourhood, which is the diffusion component (Batty, 1999). The most attractive property of CA models for simulating urban systems is that local action in such models can give rise to global forms which evolve or emerge spontaneously with no hidden hand directing the evolution of the macrostructure (Batty *et al.,* 1999). They can help in interpreting, modelling, predicting and understanding the dynamics of natural resources.

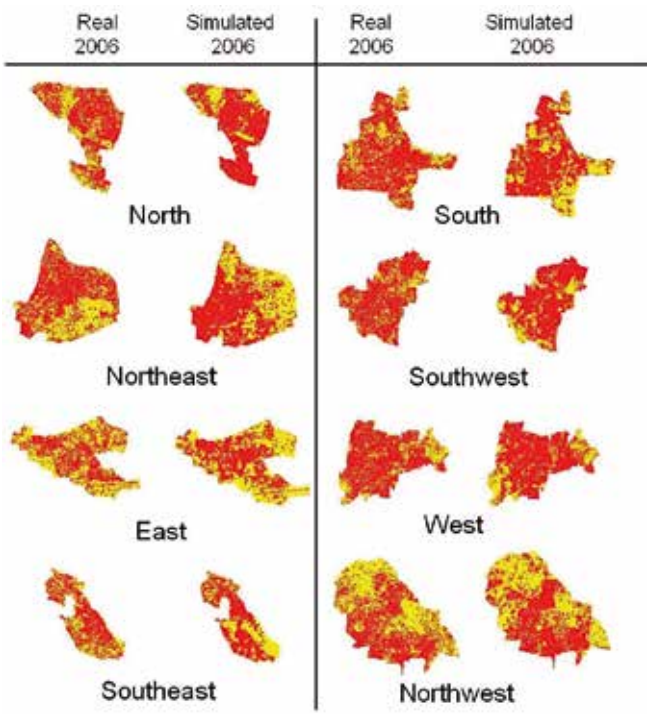

Figure 7. Real image and simulated image of 2006. Red colour indicates urban areas, yellow represents other classes (vegetation, water or open land).

Figura 7. *Imagen real e imagen simulada para 2006. El color rojo indica áreas urbanas y el amarillo representa las otras clases (vegetación, agua y campo abierto).*

Comparison of CA models with other urban process models highlights certain merits, but there are drawbacks such as (i) the relaxation of the original CA scheme may lead to the loss of fundamental characteristics of simplicity and locality, or loss in the model in which the CA component is no longer the core. (ii) CA models are not suited to define general urban CA, but are rather a method to define specific models for each situation. (iii) CA generally produces descriptive models that tell us what is happening but it does not tell us why? (iv) Data requirements depend upon the factor considered in the model and so, they are usually in opposition to flexibility (Sante *et al.,* 2010). Further research in this direction is required to focus on the drawbacks such as transition rules considering road accessibility, distance to multiple urban centres in the city, slopes, accessibility to railways, site suitability for development, population density, etc.

Conclusion

This study explores the potential of implementing cellular automata to model the historical urban growth over Bangalore from 1973 to 1992 and 1992 to 2006. The main goal was to design the model as a function of a local neighbourhood structure to minimise the input data to the model. Satellite imagery represents the medium over which the model works taking into account spatial and temporal calibration based on transition rules. Spatial calibration fits the model on a directional basis to its site specific feature, whilst temporal calibration adapts it to the urban growth dynamic change over time, producing a good spatial match between the real and simulated image data.

The technique demonstrated here was found effective in predicting urban growth and visualising it through pixels in images. Such studies are important for relating pixels in RS data and people in society for sustainable development, pollution prevention, global environmental change, and issues of human-environmental interaction at different spatial and temporal scales. The limitation of this work is that the

current CA model only takes into account land use categories, population density, and distance from the city centre. There are many other factors, such as distance from rail / roads, levels of services available in different locations, education and employment opportunities, economic flow, etc. that are major triggering factors for urbanisation in developing countries like India. Therefore, future study will involve considering agents and external factors (such as foreign direct investment flow in the city, decisions related to setting up special economic zones (SEZ), etc.) that can act as a catalyst and driving force in the expansion of cities. Land use category such as built-up land may be further classified into their different forms using very high spatial resolution imageries such as Quickbird, IKONOS, etc. The detailed land use practices may further improve the modelling result and give better prediction accuracy.

References

AlKheder, S., Wang, J., and Shan, J. 2006. Change detection -cellular automata method for urban growth model modelling. ISPRS Commission VII Mid-term Symposium *"Remote Sensing From Pixels to Processes",* Enschede, the Netherlands, 8-11 May, 2006.

AlKheder, S., Wang, J., and Shan, J. 2007. Cellular automata urban growth model calibration with genetic algorithms. *Urban Remote Sensing Joint Event,* 11-13 April, 2007, Paris, France, 1-5.

Barredo, J. I., Demicheli, L., Lavalle, C., Kasanko, M., McCormick, N. 2004. Modelling future urban scenarios in developing countries: an application case study in Lagos, Nigeria. *Environment and Planning* B: Planning and Design, 32, 65-84.

Batty, M., and Xie, Y. 1994.From cells to cities. *Environment and Planning*, B21, 531-548.

Batty, M, Xie, Y, Sun, Z. 1999. Modelling urban dynamics through GIS-based cellular automata. *Computers, Environment and Urban Systems,* 23, 205-233.

Batty, M. 2005. *Cities and Complexity: Understanding Cities with Cellular Automata, Agent-based Models, and Fractals*. The MIT Press, Cambridge, MA.

Bayarsaikhan, U., Boldgiv, B., Kim, K-R., Park, K-A., and Lee, D. 2009. Change detection and classification of land cover at Hustai National Park in Mongolia. *International Journal of Applied Earth Observation and Geoinformation,* 11, 273-280.

Census of India, 2011. Ministry of Home Affairs, Government of India.

Chen, F, Hu, Y., Peng, X., Wang, Lu., 2010, Simulation of land use/cover change based on the CLUE-S model. In *18th International Conference on Geoinformatics*, 1(5), 18-20.

Cheng, J., Masser, I., 2004. Understanding spatial and temporal process of urban growth: cellular automata modelling. *Environment and Planning B: Planning and Design,* 31, 167-194.

Clarke, K. C., and Gaydos, L. J., 1998.Loose-coupling a cellular automaton model and GIS: long-term urban growth prediction for San Francisco and Washington/Baltimore. International *Journal of Geographical Information Sciences,* 12, 699-714.

Clarke, K. C., Hoppen, S., and Gaydos, L., 1997.Aselfmodifying cellular automaton model of historical urbanization in the San Francisco Bay area. *Environment and Planning*, 24, 247-261.

Conese, C., and Maselli, F., 1992. Use of error matrices to improve area estimates with maximum likelihood classification procedures. *Remote Sensing of Environment,* 40, 113-124.

Couclelis, H., 1985. Cellular worlds: a framework for modeling micro–macro dynamics. *Environment and Planning A,* 17, 585–596.

Dietzel, C., Clarke, K. 2006. The effect of disaggregating land use categories in cellular automata during model calibration and forecasting. *Computers, Environment and Urban Systems*, 30 (1), 78–101.

Duda, R. O., Hart, P. E., and Stork, D, G. 2000. *Pattern classification*, 2nded. New York: A Wiley-Interscience Publication.

Ediriwickrema, L., Khorram, S. 1997. Hierarchical maximum-likelihood classification for improved accuracies. *IEEE Transactions on Geoscience and Remote Sensing,* 35 (4), 810-816.

Geertman, S., Hagoort, M., Ottens, H. 2007. Spatial–temporal specific neighbourhood rules for cellular automata land use modelling. *International Journal of Geographical Information Science,* 21 (5), 547–568.

Hagerstrand, T. 1967. Innovation Diffusion as a Spatial Process, Chicago, IL: University of Chicago Press.

Itami, R.M., 1994. Simulating spatial dynamics: cellular automata theory. *Landscape and Urban Planning*, 30, 24–47.

Johnson, R. A., and Wichern, D. W. 2005. *Applied Multivariate Statistical Analysis*, Pearson Education, Second Indian Reprint, New Delhi, India, 2005, pp. 591-592 and 610-611.

Lau, K.H., Kam, B.H. 2005. A cellular automata model for urban land use simulation. *Environment and Planning B: Planning and Design*, 32, 247–263.

Li, X., Yang, Q. S., Liu, X. P., 2007.Genetic algorithms for determining the parameters of the effect of disaggregating land use categories in cellular automata in urban simulation. Science in China, Series D: Earth 50(12), 1857–1866.

Li, X., Yang, Q., Liu, X., 2008. Discovering and evaluating urban signatures for simulating compact development using cellular automata. *Landscape and Urban Planning,* 86, 177–186.

Li, X., Yeh, A., 2001. Calibration of cellular automata by using neural networks for the simulation of complex urban system. *Environment and Planning A*, 33, 1445–1462.

Li, X., Yeh, A.G., 2002. Neural-network based cellular automata for simulating multiple land use changes using GIS. *International Journal of Geographical Information Sciences,* 16, 323–343.

Li, X., and Yeh, A. G. O., 2003. Error propagation and model uncertainties of cellular automata in urban simulation with GIS. In:7th International Conference on GeoCompu-

tation, 8- 10, September 2003, University of Southampton, Southampton, UK (GeoComputation CD-ROM).

Liu, S., Li, X., Shi, X., Wu, S., Liu, T., 2008. Simulating complex urban development using kernel-based non-linear cellular automata. *Ecological Modelling*, 211, 169–181.

Lillesand, T. M., and Kiefer, R. W., Remote Sensing and Image Interpretation, Fourth Edition, John Wiley and Sons: New York, 2002, ISBN 9971-51-427-3.

Pinto, N.N., Antunes, A.P., 2007. Cellular automata and urban studies: a literature survey. *Architecture, City and Environment,* 1 (3), 367–398.

Ramachandra, T.V., and Kumar, U., 2008. Wetlands of Greater Bangalore, India: Automatic Delineation through Pattern Classifiers. *Electronic Green Journal,* 1(26), 1-22.

Richards, J. A., and Jia, X., *Remote Sensing Digital Image Analysis*, Springer-Verlag: Berlin, 2006.

Sante, I. Garcia, A. M. Miranda, D., and Crecente R., 2010, Cellular automata models for the simulation of real-world urban processes: A review and analysis. *Landscape and Urban Planning,* 96, 108-122.

Silva, E.A, Clarke K.C., 2002.Calibration of the SLEUTH urban growth model for Lisbon and Porto, Portugal. *Computers, Environment and Urban Systems*, 26, 525-552.

Stevens, D., Dragicevic, S., Rothley, K., 2007.iCity: a GIS-CA modelling tool for urban planning and decision making. *Environmental Modelling & Software,* 22, 761–773.

Strahler, A. H., 1980. The use of prior probabilities in maximum likelihood classification of remotely sensed data. *Remote Sensing of Environment,* 10, 135-163.

Tobler, W., ed., 1979. Cellular geography, in Philosophy. In: Geography, Eds S Gale, G Olsson (D Reidel, Dordrecht), 379-386.

Veldkamp, A.; Fresco, L., 1996, Clue-cr: An integrated multiscale model to simulate land use change scenarios in costa rica. *Ecological Modelling,* 91, 231-248.

von Neumann, J., ed. Burks, A. W. 1966. Theory of Self-Reproducing Automata, Illinois: University of Illinois Press.

Verburg, P.H., 2010, The Clue Modelling Framework: Course Material, Amsterdam University Institute for Environmental Studies, pp. 53.

Verburg, P.H., de Koning, G., Kok, K., Veldkamp, A., Bouma, J. 1999, A spatial explicit allocation procedure for modelling the pattern of land use change based upon actual land use. *Ecological Modelling,* 116, 45–61.

Verburg, P.H. and Overmars, K.P., 2007, Dynamic Simulation of Land Use Change Trajectories with the Clue-S Model. In: *Modelling Land Use Change, Progress and Applications V*, (Eds. Koomen, Eric; Stillwell, John; Bakema, Aldrik; Scholten, H. J.), Springer, Netherlands, 90, 321-337.

Verburg, P.H., Soepboer, W., Limpiada, R., Espaldon, M.V.O., Sharifa, M., Veldkamp, A. 2002, Land use change modelling at the regional scale: the CLUE-S model. *Environmental Management*, 30, 391-405.

Verburg, P.H., Veldkamp, A. 2004, Projecting land use transitions at forest fringes in the Philippines at two spatial scales. *Landscape Ecology,* 19(1), 77-98.

Waddell, P. 2005. Introduction to urban simulation: design and development of operational models. *Handbook in Transport,* 5(2004), 203-236.

Wagner, D.F. 1997. Cellular automata and geographic information systems. *Environment and Planning B*, 24, 219–234.

White, R. and Engelen, G. 1993. Cellular Automata and Fractal Urban Form: A Cellular Modelling Approach to the Evolution of Urban Land Use Patterns. *Environment and Planning,* A(25), 1175-1199.

White, R., and Engelen, G. 1994. Cellular dynamics and GIS: modelling spatial complexity. *Geographical Systems,* 1, 237–253.

Wölfel, M., and Ekenel, H. K. 2005. *Feature Weighted Mahalanobis Distance: Improved Robustness for Gaussian Classifiers,* In Proceedings of the 13th European Signal Processing Conference: EUSIPCO, Antalya, Turkey, September, 2005.

Wolfram, S. 1984. Cellular automata: a model of complexity. *Nature*, 31, 419–424.

Wolfram, S. 1994. *Cellular automata.* In: Cellular Automata and Complexity: Collected Papers, Reading, MA: Addison Wesley.

Wolfram, S., 2002. *A New Kind of Science*. Wolfram Media, Canada.

World Urbanization Prospects, 2005.Revision, Population Division, Department of Economic and Social Affaris, UN.

Wu, F., 2002. Calibration of stochastic cellular automata: the application to rural-urban land conversions. *International Journal of Geographical Information Systems*, 16 (8), 795–818.

Wu, F., and Webster, C. J. 1998, Simulation of land development through the integration of cellular automata and multi-criteria evaluation. *Environment and Planning B,* 25, 103-126.

Wu, Ning, and Silva, E. A., 2010. Artificial intelligence solutions for Urban Land Dynamics: A Review. *Journal of Planning Literature,* 24, 246-265.

Xu, L., Li, Z., Song, H., and Yin, H. 2013, Land Use Planning for Urban Sprawl Based on the CLUE-S Model: A Case Study of Guangzhou, China. Entropy, 15, 3490-3506. Yang, Q., Li, X., Shi, X., 2008. Cellular automata for simulating land use changes based on support vector machines. *Computers & Geosciences,* 34, 592–602.

Yang, X, and Lo, C. P. 2003. Modelling urban growth and landscape changes in the Atlanta metropolitan area. *International Journal of Geographical Information Science,* 17, 463-488.

Yeh, A., Li, X., 2001. A constrained CA model for the simulation and planning of sustainable urban forms by using GIS. *Environment and Planning B: Planning and Design,* 28, 733-753.

Zheng, M., Cai, Q., and Wang, Z. 2005. *Effect of prior probabilities on maximum likelihood classifier.* In: Geoscience and Remote Sensing Symposium, IGARS'05, 25-29 July, 2005, Seoul, Korea. 2005 IEEE International, 6, 3753-3756.

Recibido: junio 2013
Revisado: septiembre 2013
Aceptado: mayo 2014
Publicado: septiembre 2014